Neurochemical Research (2023) 48:2436–2450
https://doi.org/10.1007/s11064-023-03913-z

ORIGINAL PAPER

Suberoylanilide Hydroxamic Acid Ameliorates Pain Sensitization in Central Neuropathic Pain After Spinal Cord Injury via the HDAC5/NEDD4/SCN9A Axis

Changsheng Wang[1] · Rongsheng Chen[1] · Xitian Zhu[1] · Xiaobo Zhang[1]

Received: 15 September 2022 / Revised: 13 March 2023 / Accepted: 14 March 2023 / Published online: 31 March 2023

Abstract
Pain sensitization in spinal cord injury (SCI)-induced central neuropathic pain has been a research target. Additionally, suberoylanilide hydroxamic acid (SAHA) has been reported to protect against pain hypersensitivity in central neuropathic pain. Hence, this research probed the impact of SAHA on pain sensitization in central neuropathic pain after SCI via the HDAC5/NEDD4/SCN9A axis. After SAHA treatment, SCI modeling, and gain- and loss-of-function assays, behavioral analysis was performed in mice to evaluate pain hypersensitivity and anxiety/depression-like behaviors. The enrichment of H3K27Ac in the NEDD4 promoter and the ubiquitination of SCN9A were measured with ChIP and Co-IP assays, respectively. The treatment of SAHA regained paw withdrawal threshold and paw withdrawal latency values, entry time and numbers in the center area, and entry proportion in the open arm for SCI mice, accompanied by decreases in immobility time, eating latency, thermal hyperalgesia, and mechanical ectopic pain. However, SAHA treatment did not affect the motor function of mice. SAHA treatment lowered HDAC5 expression and SCN9A protein expression in SCI mice, as well as enhanced SCN9A ubiquitination and NEDD4 expression. HDAC5 knockdown greatly increased H3K27Ac enrichment in the NEDD4 promoter. NEDD4 upregulation or HDAC5 knockdown elevated SCN9A ubiquitination but diminished SCN9A protein expression in dorsal root ganglions of SCI mice. NEDD4 silencing mitigated the improving effects of SAHA treatment on the pain hypersensitivity and anxiety/depression-like behaviors of SCI mice. SAHA suppressed HDAC5 to augment NEDD4 expression and SCN9A degradation, thereby ameliorating the pain hypersensitivity and anxiety/depression-like behaviors of SCI mice.

Keywords Spinal cord injury · Pain sensitization · Suberoylanilide hydroxamic acid · Histone deacetylase 5 · SCN9A · NEDD4 · Ubiquitination

Introduction

Spinal cord injury (SCI), mostly resulting from trauma, is a neurological dysfunction, which socioeconomically afflicts patients and the health care system and contributes to severe motor or sensory dysfunction [1, 2]. After SCI, a majority of patients suffer from chronic central neuropathic pain caused by a lesion or disease of the somatosensory system, which lacks effective treatments in the clinic [3, 4]. Hence, it is urgently needed to develop novel therapies. Recently, extensive attention has been paid to the central sensitization mechanism, where increased pain sensitivity aggravates the pain, decreases the pain threshold, and finally contributes to central neuropathic pain [5]. In addition, pain hypersensitivity is tightly associated with depression, pain-related sleep disorders, and average pain intensity [6]. Moreover, researchers have widely explored pharmaceuticals or molecules that affect pain hypersensitivity after SCI or peripheral nerve injury [7–10]. Nevertheless, existing research is far from adequate.

Histone acetylation is one of the important post-translational modifications involved in neuropathic pain, which can be regulated by the actions of histone acetyltransferases (HATs) and histone deacetylases (HDACs) [11, 12]. HDACs

Changsheng Wang and Rongsheng Chen contributed equally to this research.

✉ Changsheng Wang
wangchangsheng085@163.com

[1] Department of Spinal Surgery, First Affiliated Hospital of Fujian Medical University, No. 20 Chazhong Road, Taijiang District, Fuzhou 350005, Fujian, People's Republic of China

are a group of epigenetic regulators that are widely known as therapeutic targets for a series of diseases, including neurological diseases [13]. As a member of the class II HDACs, HDAC5 is abnormally expressed in cancers and orchestrates many cellular processes [14]. Strikingly, HDAC5 knockdown represses pain hypersensitivity in neuropathic pain of spinal cords [15]. Moreover, HDAC inhibitors have been approved for chemotherapeutic treatment [16]. More importantly, a prior study reported that an HDAC6 inhibitor reduced neuropathic pain caused by peripheral nerve injury [17]. Suberoylanilide hydroxamic acid (SAHA) is a pan-HDAC inhibitor, which suppresses class I and class II HDACs [18]. SAHA was also manifested to restrain peripheral inflammation-induced microglial activation in the hippocampus [19]. In addition, SAHA treatment was implicated to relieve thermal and mechanical pain hypersensitivity in nerve injury-induced neuropathic pain [20]. Clearly, it is very necessary to probe the mechanism of SAHA and HDAC5 on pain hypersensitivity after SCI.

Meanwhile, ubiquitination, a crucial posttranslational modification influencing protein stability, interaction partner, and biological function, has regulatory effects on numerous processes including chronic pain [21–23]. Neuronal precursor cell-expressed developmentally down-regulated 4 (NEDD4), a HECT domain E3 ligase, is mediated by HDAC5 and capable of regulating ubiquitination [24, 25]. Additionally, NEDD4 was documented to exert regulatory effects on neuropathic pain [26]. Of note, a previous report manifested that NEDD4-2 was able to decrease sodium Voltage-Gated Channel Alpha Subunit 9 (SCN9A) expression via ubiquitination in chronic post-surgical pain [27]. *Scn9a*, also named Nav1.7, is a voltage-gated sodium channel crucial in defining the threshold of the action potential and the signal propagation of sensing pain [28]. It was documented that the SCN9A channel is capable of predicting the nociceptive response of dorsal root ganglions (DRGs) [29] and its blockage functions in alleviating neuropathic pain [30].

As a result, we hypothesized that SAHA mediated the NEDD4-SCN9A axis via HDAC5 to influence central neuropathic pain sensitization after SCI and conducted a set of experiments to prove this hypothesis in the current research.

Materials and Methods

Laboratory Animals and Drug Administration

Adult male wild C57BL/6 J mice (20–30 g) were purchased from Shanghai SLAC Laboratory Animal Co., Ltd. (Shanghai, China) and underwent behavioral tests. Mice were bred with a standard cycle of 12-h light and 12-h dark, with free access to food and water. All behavioral tests were conducted at 9:00 am. Before experiments, mice were accustomed to staying in the behavior room for 30 min and the experimenters were blinded to the condition of drug administration. The animal research abided by the Animal Research: Reporting of in vivo Experiments guidelines [31] and was ratified by the Ethical Committee approval certificate (Ethnical number: IACUC FJMU 2023-0038; Date: February 24th, 2023). The experiments were designed on the principle of minimizing the quantity and pain of animals. The mice were euthanized through cervical dislocation and spinal cords were extracted for in vitro analysis. The sample size of laboratory animals was analyzed with power analysis [32] and calculated with G power software. Each test group was composed of 6 animals to ascertain the behavioral parameters.

The mice were treated and the behavioral test was carried out on the 14th day after surgery. On the day the treatment reached the best efficiency, the spinal cord for in vitro experiment was removed.

Establishment and Grouping of an SCI Mouse Model

The method referred to the previous literature [33]. Mice were pre-anesthetized with buprenorphine (0.05 mg/kg weight) and then maintained under deep anesthesia throughout the surgery with isoflurane gas (2% isoflurane mixed with 100% O_2; which was delivered via face mask at a flow velocity of 0.4 L/min). The skin at the midspinal line was cut open with the T10 spinous process as the center, and then the fascia layers and muscle layers were peeled from the T9–T11 spinous processes. After the laminectomy of T10, the mice were fixed on a stereoscopic positioning device with their spine fixed with a spine clamp. Subsequent to the use of 2% lidocaine solution (0.1 mL) at the surface of the dorsal spine, a computer-controlled impactor (Impact One Stereotaxic Impactor; Leica, Buffalo Grove, IL, USA) was employed to cause contused wounds. Mice that received only laminectomy were assigned to the sham group. A heat lamp was used to keep animals warm, accompanied by the inspection of animals during the period of recovery. Afterward, the animal was injected with a preventive dose of antibiotic (Bicillin, 10,000–30,000 units, intramuscular, Wyeth Laboratories, Collegeville, PA, USA) once a day for 5 days after surgery to control the possible infection. The animals underwent manual bladder functioning till the recovery of bladder normal function. Approximately 2 weeks after surgery, the animals were subjected to short anesthesia with 2% isoflurane to remove the skin nails.

Mice were grouped and intrathecally administrated with SAHA (Sigma-Aldrich, St. Louis, MO, USA; dissolved in 5% dimethyl sulfoxide [DMSO]) 15 min before the tests. Pregabalin (PREG, 30 mg/kg) was intraperitoneally injected into mice 3 h before the tests as an analgesic control. Drug concentration was confirmed with the following method: each mouse received a single intrathecal injection with 5

μL SAHA or intraperitoneal administration with 10 mL/kg PREG.

Mice intrathecally treated with DMSO and adenovirus empty vector [silencing (si)-negative control (NC)] 15 min before the tests were assigned as the DMSO + si-NC group (n = 6). Mice intrathecally treated with SAHA and si-NC were assigned as the SAHA + si-NC group (n = 6). Mice intrathecally treated with DMSO and NEDD4 silencing adenovirus (si-NEDD4) were arranged as the DMSO + si-NEDD4 group (n = 6). Mice intrathecally treated with SAHA and si-NEDD4 were arranged as the SAHA + si-NEDD4 group (n = 6). Recombinant adenoviruses of NEDD4 silencing were obtained from Hanbio (Shanghai, China), and each mouse was vertically injected with 20 μL si-NC or si-NEDD4 (1×10^8 plaque-forming units) in the interval of L5-6 spinous processes with microinjector.

Assessment of Basso Mouse Scale (BMS) Scores

Normal mice were placed in an open area the day before the assessment to acclimatize to the environment. Then, the motor function was assessed with BMS scores on the 1st-4th weeks after surgery, and the observation period for each score was 5 min. The motor function of mouse hind limbs was evaluated with BMS scores (0–9 scores: 0 scores represented complete paralysis, and 9 scores represented completely normal). This experiment was conducted by experimenters familiar with score rules. The BMS scores for the left and right hind limbs were calculated immediately after the observation, and the mean value was obtained.

Behavioral Analysis

These analyses were conducted on sober, unconstrained, and age-matched mice. The researchers conducted behavioral tests on mice and were blinded to the identity of the two groups. Von Frey hairs (graded from 1.4 to 26 g) were manually spread on the surface of the paw, after which PWT was selected to assess mechanical allodynia. Thermal allergic reaction within PWL was measured after thermal radiation source treatment on the surface of the paw. Meanwhile, FST, EPMT, NSFT, and OFT were supplemented to evaluate anxiety/depression-like behaviors.

Paw Withdrawal Threshold (PWT)

The mice were placed for 30 min every day in an organic glass cage with a metal net at the bottom 3 days prior to the experiment. After acclimatization, a group of von Frey hairs, the hardness of which logarithmically increased from 1.4 g, 2 g, 4 g, 6 g, 8 g, 10 g, and 15 g, to 26 g, were used, and enough force was exerted to make the filaments curved vertically for 5 s to the paw. On condition that a rapid and complete lift from the platform was observed on the hind paw, it was a favorable result. The value of PWT was confirmed by referring to the previous document [34].

Paw Withdrawal Latency (PWL)

The separate compartments for the test were placed on a 30 °C temperature-controlled glass platform, with a bore diameter-thermal radiation source generating thermal stimulus to the surface of the outward hind paw. Thermal PWL was defined with the time interval from the moment the stimulus started to the moment the paw stopped. Every 5 min, each hind paw was assessed 5 times to figure out the mean value of latency data. To minimize the tissue injury induced by extended thermal stimulus, 15 s was selected as the time to cease the latency [35].

Open Field Test (OFT)

In the period of dark, tests were carried out, and the light intensity was the same during the whole experiment. The mice were acclimated for 30 min to the test room before the operation to ensure activity stability in the experiment. A box with $100 \times 100 \times 40$ cm^3 volume was used as the box of OFT. When the experiment started, the mouse was deposited in the central area, followed by the recording of its behaviors through a video of 5-min duration. Then, 70% ethanol was utilized to completely clean the test room and eliminate any residual smell between the two operations. The entry number into the central position, the staying time in the central position, and the overall distance were recorded. Smart v.3.0 software (Panlab Harvard Apparatus, October Hill Road, Holliston, Massachusetts, USA) was applied to analyze the parameters.

Elevated Plus Maze Test (EPMT)

According to prior research [36], tests were carried out in dark, during which the density of light was controlled at the same conditions. Before tests, the mouse was made acclimated for 30 min to the test room to make sure that its activity was stable throughout the tests. The tests were carried out in a maze made up of two 110×10 cm^2 open arms and two $110 \times 10 \times 30$ cm^3 enclosed arms extending from the 10×10 cm^2 center platform at a degree of 90°. Before experiments, all mice were domesticated in the wild for 5 min by videotaping. When the experiment started, the mouse was put in the center platform towards the open arm and its activity was recorded for 5 min. The maze was completely cleaned, and the remaining smell was removed with 70% ethanol in intervals. The entry number into and staying time in the open arms, and the total distance of movement were included in the measurement parameters, which were

assessed with Smart v.3.0 software (Panlab Harvard Apparatus). The entry number in the open arms divided by the total number of entries into the open arms and the enclosed arms equaled the entry proportion in the open arms. The time in the open arms divided by the total time in the enclosed and open arms equaled the proportion of time in the open arms.

Novelty-Suppressed Feeding Test (NSFT)

Test conductions were completed during the dark phase with the controlled same light density. Before the test, the mouse was acclimated to the test room for 30 min so that the stability of activity was ensured during the test. The chamber used for NSFT was a box of $100 \times 100 \times 40$ cm^3, where a small piece of food was placed on a small piece of white paper on the core position of the bottom. After 24-h fasting, the test and timing started and the mouse was placed in the corner regions. The timing ceased at the moment the mouse began to bite. The box was completely rinsed and the residual peculiar smell was removed with 70% ethanol between two test procedures. Researchers recorded the time from the moment that the mouse was placed in the box to the moment that the mouse began to eat. If a mouse still did not have the food 10 min later, then the data were deleted [36].

Forced Swimming Test (FST)

Mice were put in a 20 cm-diameter and 60 cm-height robber cylinder where the depth of the water was 30–35 cm and the temperature of the water was 23–25 °C. The mice were forced to swim for a total of 6 min, with the first minute as the acclimation time. The time of immobility was recorded within 5 min. Water for each mouse was refreshed in case the smell influenced the next mouse. The immobility standard was that the mouse ceased struggling in the water and presented a floating state or that the mouse only had subtle limb movements to keep its head floating on the surface of the water. Two researchers blinded to groups conducted the experiments and recorded test data.

Quantitative Reverse Transcription Polymerase Chain Reaction (qRT-PCR)

Total RNA was isolated in accordance with the instructions of the Trizol method (Invitrogen, Carlsbad, CA, USA), followed by reverse transcription into cDNA with a PrimeScript RT kit (RR037A, Takara, Tokyo, Japan). Afterward, the fluorescent quantitative PCR was conducted as per the manuals of an SYBR® Premix Ex Taq™ II kit (RR820A, Takara) in a real-time fluorescence quantitative PCR instrument (ABI 7500, ABI, Foster City, CA, USA). β-actin was utilized as the internal reference and the $2^{-\Delta\Delta Ct}$ method was employed to calculate the relative expression of each target gene: $\Delta\Delta Ct = \Delta Ct$ experimental group—ΔCt control group, and $\Delta Ct = Ct$ target gene—Ct internal reference. The related primers were designed by Sangon (Shanghai, China; Table 1), and silencing (si)-HDAC1 and si-HDAC5 sequences were listed in Table 2. Each experiment was repeated 3 times.

DRG Isolation and Neurocyte Acquisition

The C57BL/6 mice were euthanatized via cervical dislocation and soaked in 750 mL/L ethanol for 3 min. Following dissection in the back, the spine of the mice was obtained and placed in a plate containing 4 °C Hank's solution. The ophthalmic scissors were utilized to cut the spine into halves along the median line of the spine, after which the spinal cord was stirred gently with micro-forceps to make the DRGs fall off like a string of beads. Each ganglion was placed in a centrifuge tube. The nerve root was cut off and an appropriate amount of 1.25 g/L Type I collagenase was added, followed by 90-min shaking at 37 °C. Subsequent to centrifugation, the Type I collagenase was removed, after which 2.5 g/L trypsin was added and the sample underwent 15-min shaking at 37 °C.

After the digestion, centrifugation was conducted with the removal of the supernatant. Thereafter, Dulbecco's Modified Eagle Medium encompassing 100 mL/L fetal bovine serum, 10 mL/L penicillin and streptomycin, and 100 μg/L nerve growth factor was added to resuspend the sample. The neurocytes were repeatedly titrated to form single-cell suspensions with a sterile glass micro-tube and then seeded in the culture dish which was pre-coated with 10 mL/L Poly (ethylene imine) solution and 5 μg/mL laminin ahead of 1 day. Last, the neurocytes were cultured in a 37 °C incubator with 50 mL/L CO_2.

Identification and Purity Determination of Neurocytes

Following 24-h incubation, the mediums were all renewed, followed by medium replacement every 3 days. Different

Table 1 Primer sequences for qRT-PCR

Genes	Sequences
SCN9A-F	GCACTCCTTATTCAGCATGC
SCN9A-R	AGACATTGCCCAGGTCCACA
β-actin-F	CTCGTCGTCGACAACGGCTCC
β-actin-R	TTTTCTCCATGTCGTCCCAGTT

qRT-PCR quantitative reverse transcription polymerase chain reaction, *F* forward, *R* reverse, *SCN9A* sodium voltage-gated channel alpha subunit 9

Table 2 siRNA sequences

	SS sequence	AS sequence
si-HDAC1	CAGUGAUGACUACAUUAAAUU	UUUAAUGUAGUCAUCACUGUG
si-HDAC5	GGUAGAUAUAGUUCUAGAAUA	UUCUAGAACUAUAUCUACCCU
si-NEDD4	GGAUAAAGACUACUACUUAAU	UAAGUAGUAGUCUUUAUCCUA

Si small interfering, *HDAC* histone deacetylase

phases of neurocytes were observed under an inverted microscope, and their morphological changes were recorded. Neurocytes on the 7th day of culture were washed 3 times with 0.01 mol/L phosphate-buffered saline (PBS) after the removal of the medium, followed by 40-min fixing with 40 g/L paraformaldehyde at room temperature and 3 washes with 0.01 mol/L PBS (5 min each time). Afterward, neurocytes were reacted with 1 mL/L Triton liquid for 30 min at room temperature and rinsed with 0.01 mol/L PBS 3 times (5 min each time). After 30-min blocking with 100 mL/L normal goat serum (NGS), the NGS was removed, and cells were probed overnight at 4 °C with neuron-specific enolase (NSE) monoclonal antibodies. After primary antibodies recycling and 3 washes with 0.01 mol/L PBS, the cells were incubated with red fluorescence-labeled goat anti-mouse Immunoglobulin G (IgG) for 1 h at room temperature in dark. Next, the secondary antibodies were removed and cells underwent 3 washes with 0.01 mol/L PBS, after which cells underwent 5-min reaction with Hoechst 33,342 staining fluid at room temperature avoiding light. Following 3 times of 0.01 mol/L PBS rinsing, cell slides were taken out from the culture dish and mounted with anti-fluorescence quenching agent. Image J software was applied to count the cells, followed by the determination of the purity of neurocytes (data not shown).

Chromatin Immunoprecipitation (ChIP) Assay

An EZ-ChIP™ kit (Millipore, Billerica, MA, USA) was used for the ChIP assay. Thirty-six h after culture, cells were fixed with 1% methanol, evenly mixed with 2.5 M glycine, and placed at normal temperature for 5 min, followed by the termination of cross-linking. After PBS washing, cells were scraped and collected, followed by centrifugation and acquisition of cell precipitates, which were resuspended in cell lysis to reach a final cell concentration of 2×10^6 cells/200 μL. After the addition of protease inhibitor mixture, samples were subjected to 5-min centrifugation at 5000*g*, resuspending with nuclei isolation buffer, and 10-min lysing in an ice-water bath. Samples were broken with ultrasound to 200–1000-bp chromatin fragments. Subsequent to 10 min of centrifugation (4 °C, 14,000*g*), the supernatants were obtained. Every 100 μL supernatant (DNA fragments) was supplemented with 900 μL ChIP dilution buffer and 20 μL of 50 × protease inhibitor cocktail. After further addition of 60 μL protein A agarose/salmon sperm DNA, the supernatants were completely mixed at 4 °C for 1 h and allowed to stand for 10 min at the same temperature, followed by 1-min centrifugation at 700 g. Next, 20 μL supernatants were attained as Input. In the experimental and NC groups, supernatants were respectively probed with 1 μL H3K27ac rabbit antibodies (b4729, Abcam, Cambridge, UK) and 1 μL IgG rabbit antibodies (#5946, Cell Signaling Technologies, Beverly, MA, USA) coupled with beads, followed by centrifugation. Each tube was eluted twice with 250 μL ChIP wash buffer and de-cross-linked with 20 μL of 5 M NaCl, after which DNAs were recycled and purified with a DNA purification kit (Beyotime, Shanghai, China). In the end, qRT-PCR was conducted.

Western Blot Assay

Radio-Immunoprecipitation assay lysis containing phenylmethylsulfonyl fluoride was utilized to extract the total protein of tissues and cells, after which samples were cultured on ice for 30 min and received 10-min centrifugation at 4 °C and 8000*g*, with the supernatant obtained. A bicinchoninic acid kit was employed to detect the concentration of total proteins. Afterward, 50 μg proteins were dissolved in 2 × sodium dodecyl sulfate (SDS) loading buffer, boiled for 5 min at 100 °C, and subjected to SDS–polyacrylamide gel electrophoresis. Next, proteins were transferred to a polyvinylidene fluoride membrane through a wet-transferring method and then blocked for 1 h in 5% skimmed milk powder. Afterward, the membrane was probed overnight with diluted primary antibodies (Abcam) against SCN9A (ab65167, 1:1000), HDAC1 (ab109411, 1:1000), HDAC5 (ab55403, 1:1000), NEDD4 (ab240753, 1:1000), and beta-ACTIN (ab8226, 1:10,000) at 4 °C. Subsequent to washing, horseradish peroxidase-labeled secondary IgG antibodies (1:5000, ab205718, Abcam) were added and cultured with the membrane for 2 h at room temperature. The membrane was developed with electrochemiluminescence and scanned and analyzed on a gel imager. Image J analysis software was adopted to quantify the gray value of protein bands, with beta-ACTIN as the internal reference. The experiment was repeated 3 times.

Ubiquitination Measurement

Hemagglutinin (HA)-ubiquitin (Ub) expressed plasmids were transiently transfected into cells for 24 h alone or in combination with co-transfection with NEDD4-myc vectors. After PBS washing, samples were boiled in 200 µL denaturing buffer (150 mM Tris–HCl [pH 7.4] and 1% SDS) for 10 min. The lysates were prepared with lysis buffer and then immunoprecipitated using 1 µg anti-SCN9A antibodies, after which anti-HA or anti-SCN9A antibodies were utilized for western blot assay of SCN9A ubiquitination degree.

Statistical Analysis

GraphPad prism8 software was applied for statistical analysis and all data were presented in the form of mean ± standard deviation. The student two-tailed test was employed to compare two groups and one-way analysis of variance (ANOVA) to compare multiple groups. For post hoc multiple comparisons, Tukey's test was applied. In the special instructions, two-way ANOVA was adopted to confirm the *P* value among multiple groups, with the least significant difference test for post hoc multiple comparisons. $P < 0.05$ was regarded as a statistically significant difference.

Results

Successful Development of the SCI Mouse Model

First, the SCI mouse model was established. Since the first day after SCI, BMS scores of SCI mice were markedly declined and lower than that of sham-operated mice within 4 weeks (Fig. 1B). Additionally, compared with sham-operated mice, SCI mice had a strong sense of mechanical ectopic pain (Fig. 1C) and thermal hyperalgesia (Fig. 1D). There existed no significant differences in PWT and PWL of contralateral paws in mice (Supplementary Fig. 1A, B). Afterward, anxiety/depression-like behaviors in SCI mice were evaluated. In the OFT, a notable reduction in entry number and time into the central area of SCI mice was observed in contrast to sham-operated mice on the 7th day (Fig. 1E, F). In the EPMT, SCI mice also exhibited markedly decreased entering proportion in the open arms on the 7th day (Fig. 1G, H). The NSFT was able to reflect the anxiety/depression-like behaviors of mice by forcing them to eat and escape. By the 21st day after SCI, the feeding latency of SCI mice was distinctly longer than that of sham-operated mice (Fig. 1I). In the FST, the immobility time of mice was dramatically prolonged on the 21st day after SCI modeling (Fig. 1J). Moreover, the motor ability of SCI mice was not affected (Fig. 1K). These results indicated that SCI mice displayed pain hypersensitivity while having anxiety/depression-like behaviors within 2–3 weeks.

SAHA Relieved Pain Hypersensitivity of SCI Mice

After the successful establishment of SCI in mice and confirmation of the presence of hypersensitivity to mechanical and thermal pain in SCI mice, the dosage-reaction curve exhibited anti-pain hypersensitivity activity in the ipsilateral paws of SCI mice and no influence on the contralateral paws (Fig. 2B). Three µg SAHA had some degree of alleviatory effects on SCI-induced pain hypersensitivity. However, 10 µg SAHA exhibited a similar effect to PREG (Fig. 2B). After the injection of 10 µg SAHA into the cerebrospinal membrane, the generated effect on anti-pain hypersensitivity was similar to that of PREG (Fig. 2B, E). Time curves were investigated at the minimum dosage (3 µg, Fig. 2C, F) and the maximum effective dosage (10 µg, Fig. 2D, G) which increased the pain threshold. The effect of SAHA reached the peak value 60 min after drug administration, lasted till 90 min, and then vanished after 120 min. Similar time course curves were also observed in the curves obtained under the minimum and maximum effective dosage (Fig. 2C, D, F–G). Therefore, corresponding experiments were conducted 2 weeks after the model induction, 60 min after drug administration, and in the ipsilateral paws.

SAHA Ameliorated Anxiety/Depression-like Behaviors of SCI Mice

We then probed whether SAHA relieved the anxiety/depression-like behaviors of SCI mice. In the OFT, the number and time of entries in the center area of SCI mice markedly decreased versus sham-operated mice in the 1st week whilst SAHA-treated SCI mice showed little distinct changes versus sham-operated mice (Fig. 3B, C). In EPMT, the entry proportion in the open arms was also conspicuously reduced in the 1st week after SCI modeling while no evident difference was observed between SAHA-treated SCI mice and sham-operated mice (Fig. 3D, E). In the NSFT, in the 3rd week after SCI, the feeding latency of SCI mice was memorably longer than that of sham-operated mice, which was nullified by SAHA treatment (Fig. 3F). In FST, mice experienced prolonged immobility time on the 21st day after SCI, whereas SAHA treatment reversed this result (Fig. 3G). Additionally, the motor ability of SCI mice was not afflicted by the treatment of SAHA (Fig. 3H). These data illustrated the mitigating effects of SAHA on anxiety/depression-like behaviors of SCI mice.

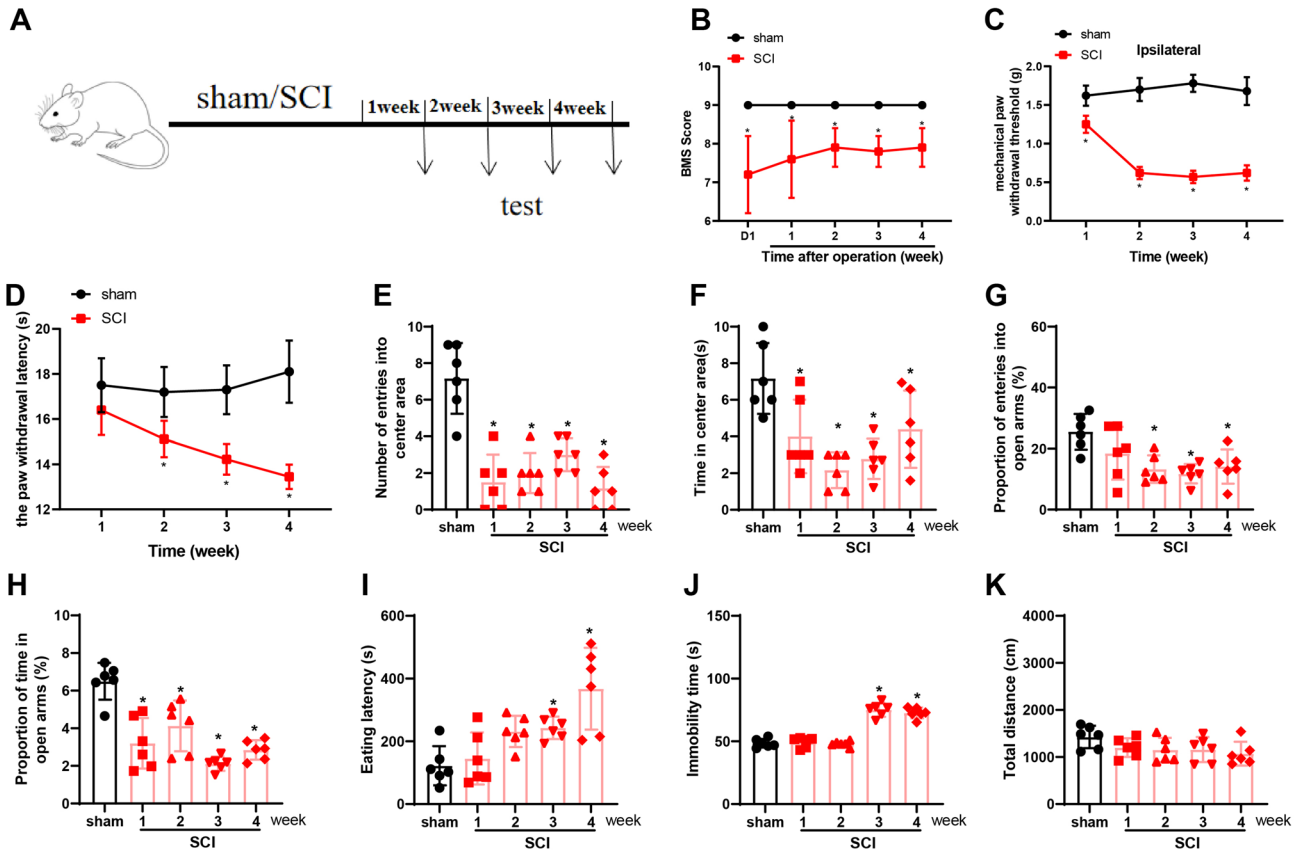

Fig. 1 SCI mice show pain hypersensitivity and anxiety/depression-like behaviors. (**A**) Treatments of mice in different groups; (**B**) The changes of BMS scores from the 1st day to the 4th week after T10 SCI (n = 6) or sham operation (n = 6), $^{*}P < 0.05$ versus the sham group. Two-way analysis of variance was adopted to confirm *P* value and LSD to conduct the post hoc multiple comparisons; (**C**, **D**) The conspicuously decreased ipsilateral PWT (**C**) and PWL (**D**) of mice after SCI; $^{*}P < 0.05$ versus the sham group. Two-way analysis of variance was adopted to confirm *P* value and LSD to conduct the post hoc multiple comparisons; (**E**, **F**) The notably reduced number and time of entries in the center area of mice after SCI in OFT; (**G**, **H**) The remarkably lowered proportion of number and time of entries in the open arms of mice after SCI in EPMT test; (**I**, **J**) The evidently increased time of eating latency of SCI mice in NSFT (**I**) and time of immobility of SCI mice in FST (**J**); (**K**) The little obvious difference in total movement distance of SCI mice in OFT. N = 6. Except for the special instructions, one-way analysis of variance was applied to confirm the *P* value and Tukey's test to validate post hoc multiple comparisons. *SCI* spinal cord injury, *BMS* Basso mouse scale, *N* number, *LSD* least significant difference, *PWT* paw withdrawal threshold, *PWL* paw withdrawal latency, *OFT* open field test, *EPMT* elevated plus maze test, *NSFT* novelty-suppressed feeding test, *OFT* open field test

SAHA Regulated HDAC5-Mediated NEDD4 and SCN9A Expression in SCI Mice

Earlier research found that *Scn9a*-encoded specific expression of Nav1.7 takes a part in sodium ion transportation and neuropathic pain in neurons [30, 37, 38]. Additionally, the SCN9A channel accelerated stimuli, initiating pain-signaling DRG firing and motivating the release of neurotransmitters at the first synapse in the spinal cord [29]. Therefore, to probe the potential role of SCN9A in the ameliorating effects of SAHA on SCI mice, SCN9A expression in the ipsilateral injured SCs from sham-operated and SCI mice within 4 weeks after surgery was monitored by qRT-PCR and western blot assay. Results demonstrated that the mRNA level of SCN9A showed no marked changes but the protein level was substantially enhanced after SCI modeling, with the highest protein expression in the 2nd week after SCI modeling (Fig. 4B, C). Next, SCN9A expression was also measured in the ipsilateral injured SC of sham-operated mice, SCI mice, and SAHA-treated SCI mice in the 2nd week after surgery. The results showed insignificant differences in the mRNA expression of SCN9A among these groups (Fig. 4D). However, the protein expression of SCN9A was evidently reduced in SAHA-treated mice compared with sham-operated and SCI mice (Fig. 4E). All these findings revealed that SCN9A might be involved in the ameliorating effects of SAHA on pain hypersensitivity and anxiety/depression-like behaviors of SCI mice. Meanwhile, the little conspicuous changes in SCN9A mRNA expression after SAHA

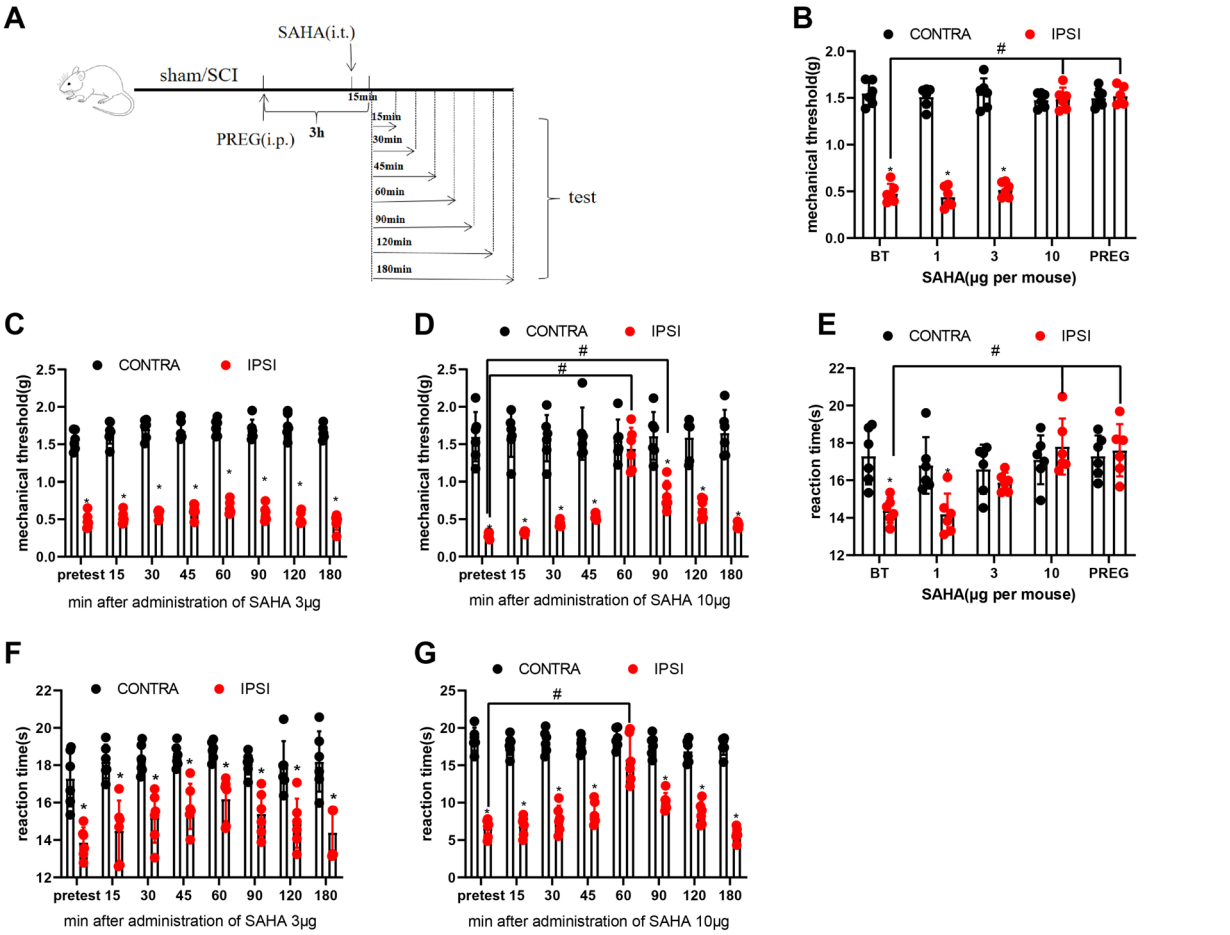

Fig. 2 SAHA eases pain hypersensitivity in SCI mice. (**A**) Treatments for different groups of mice; (**B**) Von Frey test to assess the influence of different dosages of SAHA (1–10 μg, intrathecally injected into mice) on mouse PWT, with PREG (30 mg/kg, intraperitoneally injected into mice) as the control drug. $^{*}P<0.05$ vs. contra; $^{\#}P<0.05$ vs. ipsi before treatment; (**C**, **D**) The time curve of anti-pain hypersensitivity after intrathecal administration with 3 μg (**C**) or 10 μg (**D**) drug in each mouse; (**E**) PWL detection of mice treated with different dosages of SAHA; (**F**, **G**) PWL detection of mice after intrathecal administration with 3 μg (**F**) or 10 μg (**G**) drug. N = 6. Two-way analysis of variance was adopted to confirm the *P* value and LSD to conduct the post hoc multiple comparisons. *SAHA* suberoylanilide hydroxamic acid, *SCI* spinal cord injury, *PWT* paw withdrawal threshold, *PWL* paw withdrawal latency, *PREG* pregabalin, *Contra* contralateral, *Ipsi* ipsilateral, *N* number

treatment implicated that SAHA might impact SCI mice via post-translational modification.

It has been known that NEDD4-2 negatively modulated Navs through ubiquitination [27, 39]. Therefore, the expression of ubiquitination-associated proteins was detected. It was found that after SAHA treatment, NEDD4 and Itchy E3 Ubiquitin Protein Ligase (ITCH) expression was prominently increased in SCI mice while other ubiquitination-associated proteins (SMURF2 and MDM2) insignificantly changed (Supplementary Fig. 1C–F). Moreover, Ubibrowser database (http://ubibrowser.ncpsb.org.cn) predication results further showed that SCN9A was modified by E3 ubiquitin ligase NEDD4 (Fig. 4F). In the current research, it was further investigated whether HDAC and ubiquitination-associated proteins were implicated in the relieving effects of SAHA on pain hypersensitivity and anxiety/depression-like behaviors of SCI mice. Considering the fact that SAHA is an HDAC inhibitor, we conjectured the potential involvement of HDACs in the improving impacts of SAHA on pain hypersensitivity and anxiety/depression-like behaviors of SCI mice. Thereby, it was observed via western blot assay that HDAC1 and HDAC5 expression was all dramatically enhanced in SCI mice in comparison with sham-operated mice whilst there was no observable difference between SAHA-treated SCI mice and sham-operated mice (Fig. 4G, H). ChIP assay manifested that, after the knockdown of HDAC1 or HDAC5, H3K27Ac was enriched to some degree in the promoter region of NEDD4 in SCI mice (Fig. 4I). Additionally, NEDD4 expression was substantially downregulated in SCI mice but not remarkably changed in

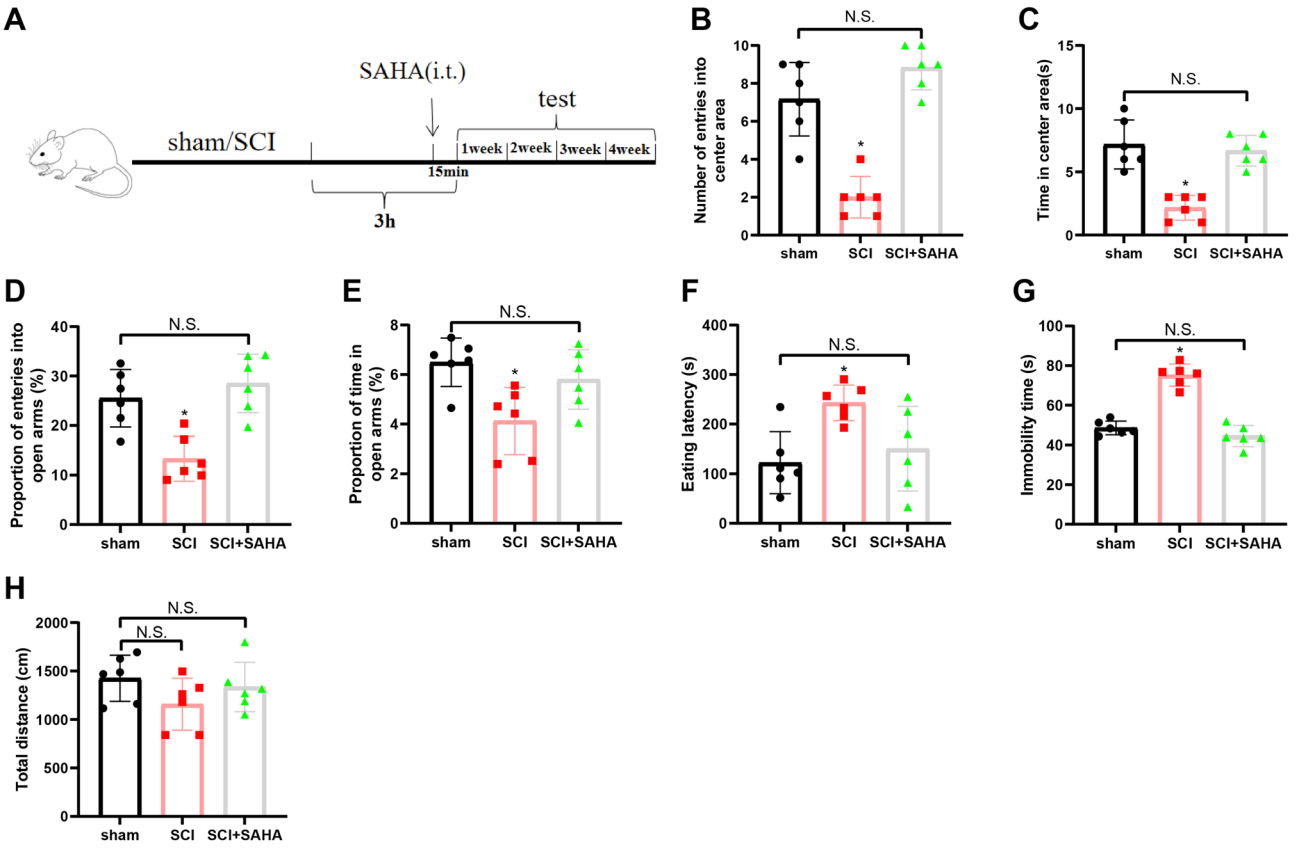

Fig. 3 SAHA alleviates anxiety/depression-like behaviors of SCI mice. (**A**) Treatments for mice in different groups; (**B**, **C**) The notably reduced number and time of mouse entries in the center area in OFT after SCI; (**D**, **E**) The evidently lowered proportion of SCI mouse entries in the open arms in EPMT; (**F**, **G**) The significantly increased time of both NSFT (**F**) and FST (**G**) in SCI mice; (**H**) No distinct differences in total movement distance of SCI mice in OFT. $^{*}P < 0.05$ versus the sham group. N = 6. Except for special instructions, one-way analysis of variance was applied to confirm the *P* value and Tukey's test to validate post hoc multiple comparisons. *SAHA* suberoylanilide hydroxamic acid, *SCI* spinal cord injury, *OFT* open field test, *EPMT* elevated plus maze test, *NSFT* novelty-suppressed feeding test, *N* number

SAHA-treated SCI mice versus sham-operated mice (Fig. 4J, K). Western blot assay results documented that after HDAC5 knockdown, NEDD4 expression in SCI mice was evidently augmented, consistent with the trends induced by SAHA treatment. However, the knockdown of HDAC1 did not alter NEDD4 expression in SCI mice (Fig. 4L, M). These findings suggested that SAHA might alter the expression of NEDD4-SCN9A mediated by HDAC5 in SCI mice.

NEDD4 Knockdown Counteracted the Repression of Pain Hypersensitivity and Anxiety/Depression-like Behaviors of SCI Mice Triggered by SAHA Treatment

To further prove that SAHA alleviated pain hypersensitivity and anxiety/depression-like behaviors of SCI mice via HDAC5-mediated the NEDD4-SCN9A axis, the mice were intrathecally treated with SAHA and si-NEDD4 after SCI operation. In the OFT, the number and time of entries in the center area of SAHA-treated SCI mice were evidently reduced after si-NEDD4 treatment (Fig. 5B, C). In the EPMT test, the proportion of entries in the open arms of mice was conspicuously lowered in SAHA-treated SCI mice following si-NEDD4 treatment on the 14th day after surgery (Fig. 5D, E). In the NSFT, SCI mice treated with SAHA + si-NC had a distinctly shorter eating latency than SCI mice treated with DMSO + si-NC, which was contrary to SCI mice treated with SAHA + si-NEDD4 compared to SCI mice treated with SAHA + si-NC mice on the 21st day after SCI (Fig. 5F). The FST results manifested that 21 days after SCI, the immobility time of SCI mice treated with SAHA + si-NC was markedly decreased in contrast to SCI mice treated with DMSO + si-NC, whereas SCI mice treated with SAHA + si-NEDD4 presented an opposite trend versus SCI mice treated with SAHA + si-NC group (Fig. 5G). Moreover, the treatment of SAHA or si-NEDD4 did not influence the motor capability of SCI mice (Fig. 5H). Taken together, SAHA modulated the NEDD4-SCN9A axis via

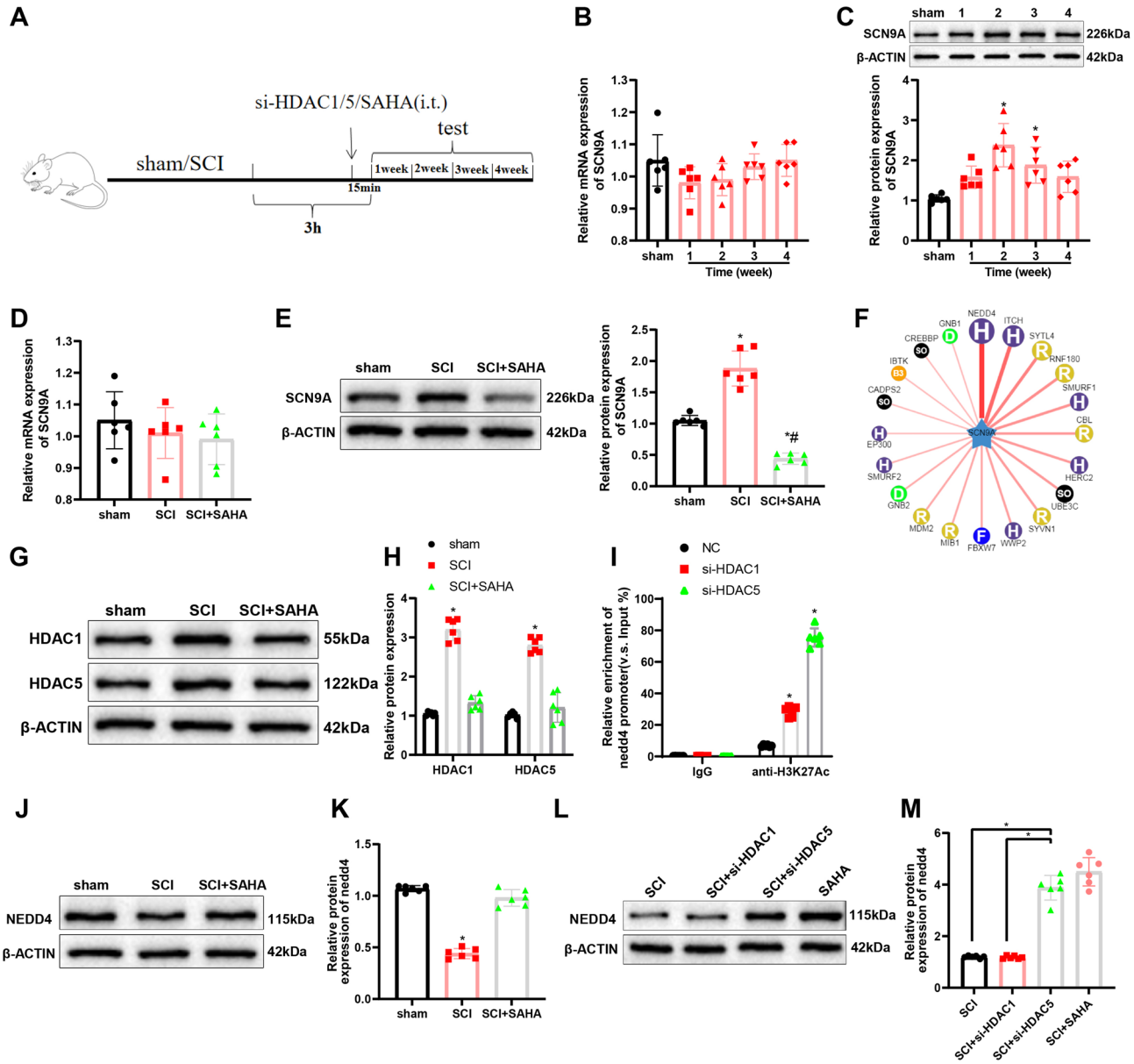

Fig. 4 SAHA mediates NEDD4-SCN9A expression by downregulating HDAC5. (**A**) Treatment for different groups of mice; (**B**, **C**) qRT-PCR (B) and western blot assay (**C**) to measure the mRNA and protein levels of SCN9A in the ipsilateral injured SCs of mice from the 1st to the 4th week after sham operation and SCI surgery; (**D**, **E**) qRT-PCR (**D**) and western blot assay (**E**) to test the mRNA and protein expression of SCN9A in the ipsilateral injured SCs of mice in the 2nd week after sham operation and PCI surgery and those of mice intrathecal injected with 10 μg SAHA in the 2nd week after SCI surgery. $^{*}P<0.05$ versus the sham group; $^{\#}P<0.05$ versus the SCI group; (**F**) Bioinformatics analysis of SCN9A-related ubiquitin-associated proteins; (**G**, **H**) Western blot assay to determine the protein expression of HDAC1 and HDAC5 in the mice from (**D**, **E**). $^{*}P<0.05$ versus the sham group; (**I**) ChIP to detect the enrichment level of H3K27Ac in the promoter region of NEDD4 in the ipsilateral DRGs of mice intravenously injected with si-HDAC1 or si-HDAC5 via tail vein in the 2nd week after SCI surgery. $^{*}P<0.05$ versus the IgG group. Data were obtained from 6 independently repeated experiments; (**J**, **K**) Western blot assay to examine the protein expression of NEDD4 in the mice from (**D**, **E**). $^{*}P<0.05$ versus the sham group; (**L**, **M**) Western blot assay to test NEDD4 protein expression in the ipsilateral injured spinal cords from untreated SCI mice and si-HDAC1/si-HDAC5-transfected and SAHA-treated SCI mice in the 2nd week after SCI surgery. $^{*}P<0.05$ versus the SCI group. N = 6. Except for the special instructions, one-way analysis of variance was applied to confirm the *P* value and Tukey's test to conduct post hoc multiple comparisons. *SAHA* suberoylanilide hydroxamic acid, *NEDD* neuronal precursor cell-expressed developmentally downregulated, *HDAC* histone deacetylase, *SCN9A* sodium voltage-gated channel alpha subunit 9, *SCI* spinal cord injury, *qRT-PCR* quantitative reverse transcription polymerase chain reaction, *mRNA* messenger RNA, *ChIP* chromatin immunoprecipitation, *DRG* dorsal root ganglion, *IgG* Immunoglobulin G, *N* number

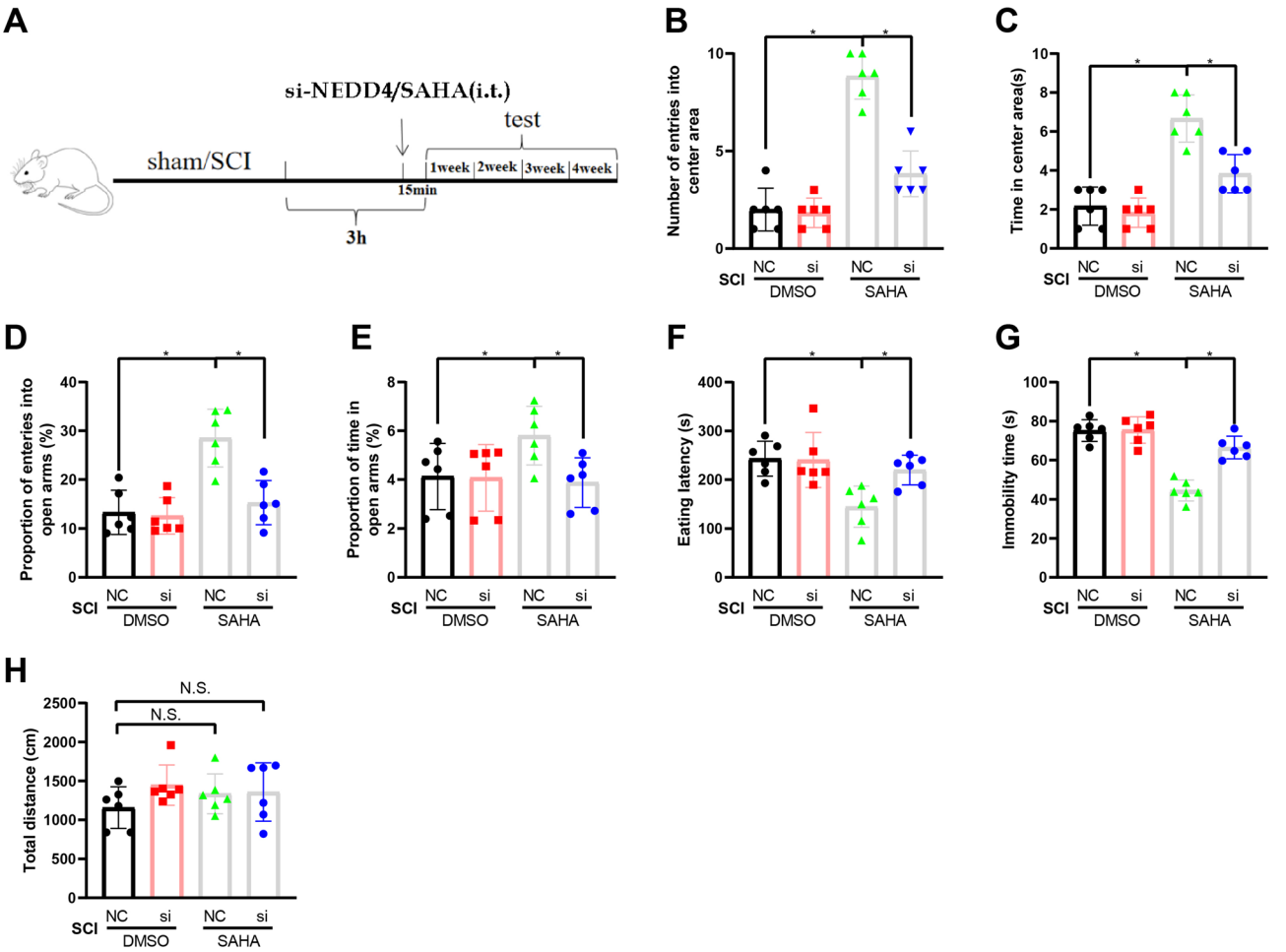

Fig. 5 The knockdown of NEDD4 abrogates the alleviatory impact of SAHA treatment on pain hypersensitivity and anxiety/depression-like behaviors of SCI mice. (**A**) Treatments of mice in different groups; (**B**, **C**) OFT to check the number and time of entries in the center area of SCI mice after treatment with SAHA and si-NEDD4 (i.t.); (**D**, **E**) EPMT to detect the number and time of entries in the open arms of SCI mice after treatment with SAHA and si-NEDD4 (i.t.); (**F**, **G**) The eating latency (**F**) and immobility time (**G**) of SCI mice after treatment with SAHA and si-NEDD4 (i.t.); (**H**) OFT to calculate the total movement distance of SCI mice after treatment with SAHA and si-NEDD4 (i.t.). $^{*}P<0.05$. N = 6. Except for the special instructions, one-way analysis of variance was applied to confirm the *P* value and Tukey's test to conduct post hoc multiple comparisons. *SAHA* suberoylanilide hydroxamic acid, *NEDD* neuronal precursor cell-expressed developmentally down-regulated, *SCI* spinal cord injury, *OFT* open field test, *EPMT* elevated plus maze test, *NSFT* novelty-suppressed feeding test, *N* number

HDAC5 to relieve pain hypersensitivity and anxiety/depression-like behaviors of SCI mice.

SAHA Facilitated Ubiquitination of SCN9A by Upregulating HDAC5-Mediated NEDD4

To further verify whether NEDD4 influenced SCN9A expression via ubiquitination to participate in the impacts of SAHA on pain hypersensitivity and anxiety/depression-like behaviors of SCI mice. Co-IP assay data showed that the ubiquitination of SCN9A was apparently increased in ipsilateral (injury) DRGs of SCI mice treated with SAHA compared with the untreated cells (Fig. 6A). In addition, ubiquitination was enhanced in a gradient along with the increase in the dosage of SAHA (Fig. 6B). Additionally, NEDD4 overexpression augmented SCN9A ubiquitination to a certain degree (Fig. 6C), accompanied by the remarkably diminished protein level of SCN9A (Fig. 6D). Meanwhile, ipsilateral DRGs (injury) of SCI mice were transfected with si-HDAC5 or si-HDAC1 plasmids. The results exhibited that the knockdown of HDAC1 slightly increased SCN9A ubiquitination in cells (Fig. 6E). Meanwhile, HDAC5 knockdown contributed to the prominent enhancement in SCN9A ubiquitination in ipsilateral DRGs of SCI mice, which was similar to the function of SAHA treatment (Fig. 6F). All these observations reflected that SAHA might inhibit HDAC5 expression to activate

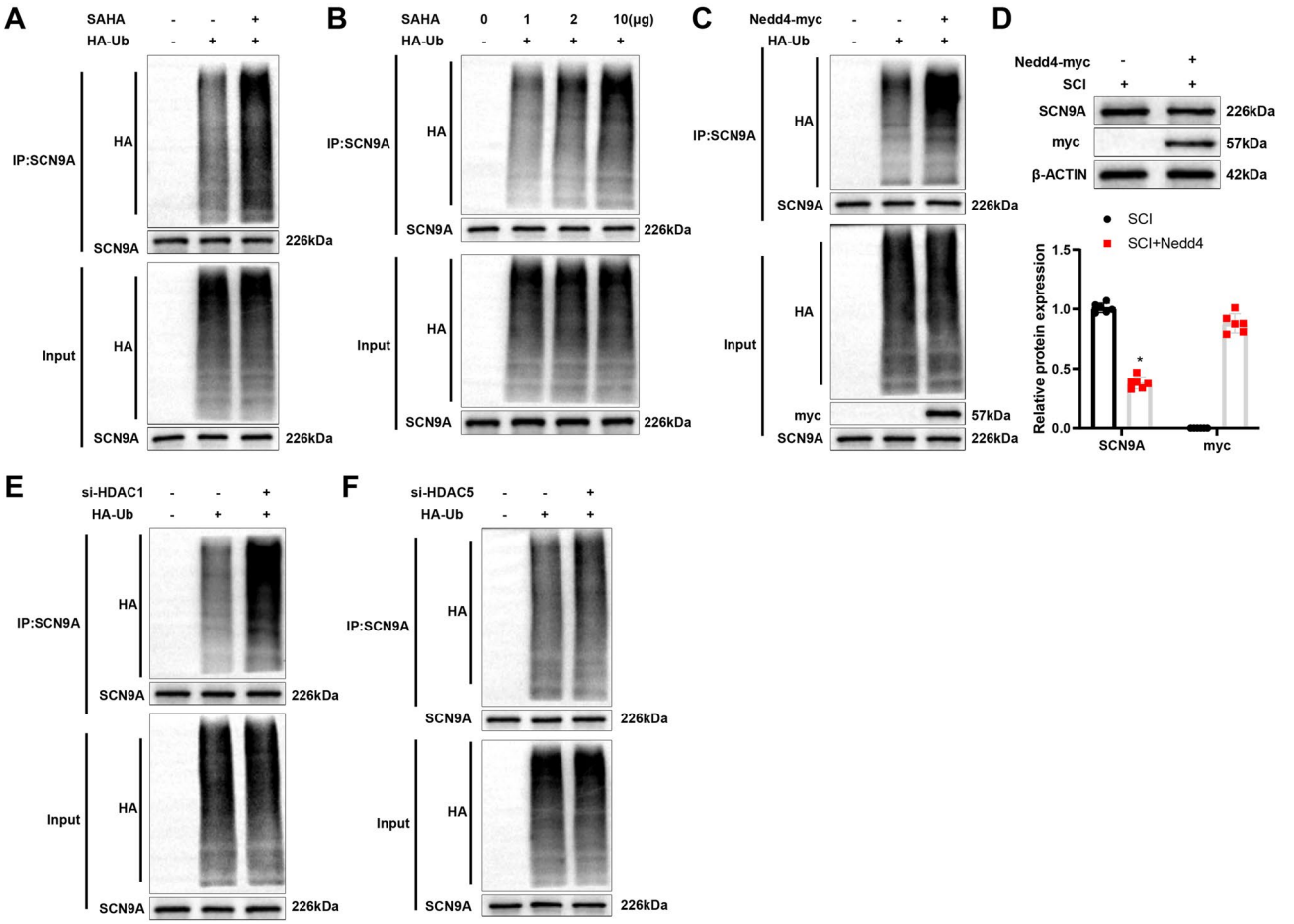

Fig. 6 SAHA promotes NEDD4 expression via HDAC5 to motivate SCN9A ubiquitination. (**A**) The ubiquitination measurement subsequent to twenty-four h transfection of HA-Ub into ipsilateral DRGs of SCI mice 2 weeks after operation; (**B**) The 1-h culture with different dosages (1–10 μg) of SAHA after 24-h HA-Ub transfection in cells of (**A**); (**C**) SCN9A ubiquitination detection after NEDD4-myc or empty myc vectors were co-transfected for 24 h with HA-Ub into cells of (**A**); (**D**) Western blot assay to detect SCN9A expression of cells of (**C**); (**E**, **F**) SCN9A ubiquitination determination after HA-Ub was co-transfected for 24 h with si-HDAC1 (**E**) or si-HDAC5 (**F**) into cells of (**A**). $^{*}P < 0.05$ versus the SCI group. Data were obtained from 6 independently repeated experiments. Except for the special instructions, one-way analysis of variance was applied to confirm the *P* value and Tukey's test to validate post hoc multiple comparisons. *SAHA* suberoylanilide hydroxamic acid, *NEDD* neuronal precursor cell-expressed developmentally down-regulated, *HDAC* histone deacetylase, *SCN9A* sodium voltage-gated channel alpha subunit 9, *HA-Ub* HA-tagged ubiquitin

NEDD4 transcription, thus promoting the ubiquitination of SCN9A to largely degrade SCN9A in DRGs of SCI mice.

Discussion

A large proportion of SCI patients experience central neuropathic pain and are afflicted by clinical pain behaviors including allodynia and hyperalgesia, which negatively influence the life quality of patients and require more adequate treatments [40]. It was reported in a prior study that central sensitization in the uninjured spinal cord region might cause central neuropathic pain after SCI [41] and that rats with spared nerve injury rats presented central hypersensitivity [42]. In addition, previous research disclosed that patients with central sensitization had a relatively greater level of anxiety and depression compared with those with other forms of pain [43]. As a result, in this research, the related regulatory mechanism in central neuropathic pain after SCI was explored in terms of pain hypersensitivity and anxiety/depression-like behaviors of mice and it was discovered that SAHA decreased HDAC5 expression to enhance NEDD4 acetylation and SCN9A ubiquitination, thus ameliorating pain hypersensitivity and anxiety/depression-like behaviors of SCI mice.

HDAC5, a mechanosensitive histone deacetylase required for loading-induced bone formation [44], was reported to increase apoptosis, inflammation, and endoplasmic reticulum stress to facilitate SCI [45]. It was also manifested that the nuclear exclusion of HDAC5 assisted in analgesia in

peripheral neuropathic pain [46]. Furthermore, HDAC5 inhibition protected against pain hypersensitivity and anxiety/depression-like behaviors in mice [15, 47]. HDAC inhibitors including SAHA are put into clinical use or under investigation for their therapeutic effects [48]. SAHA was discovered to attenuate neuropathic pain and promote autophagy of astrocytes and neurons in the spinal dorsal horn of rats [49]. It was also illustrated that the administration of SAHA in the spinal dorsal horn and DRGs participated in the alleviation of bone cancer pain [50]. It's worth noting that, the proper dosage of SAHA administration was discovered to increase the pain threshold and diminish thermal and mechanical hypersensitivity in nerve-injured mice [20]. Likewise, our results reflected that SAHA treatment attenuated mechanical ectopic pain and thermal hyperalgesia in SCI mice. Based on the aforementioned close linkage between central sensitization and anxiety/depression-like behaviors, the behavioral tests were planned to assess the impact of SAHA on anxiety/depression-like behaviors in SCI mice. It was elucidated in our experiments that, after SAHA treatment, the time and number of entries in the core area and the entry proportion in the open arms were efficiently recovered whilst immobility time and eating latency were shortened for SCI mice, which indicated the relieving impact of SAHA on anxiety/depression-like behaviors during SCI. Intriguingly, similar trends were found in two earlier studies that SAHA protected against depression-like behaviors in mice and that inhibition of HDACs with the use of SAHA functioned in dispelling fear (the therapeutic target for anxiety) [51, 52]. In conclusion, SAHA might be an inhibitor of pain hypersensitivity and anxiety/depression-like behaviors following SCI.

SCN9A, a known voltage-gated sodium channel, is recognized to be responsible for sensitivity to pain [53]. Interestingly, there was research unveiling that the SCN9A channel is altered in neuropathic pain and associated with the regulation of central hyperexcitability [54–57]. It was assumed that SCN9A might be implicated in the influence of SAHA on pain sensitization after SCI. Given that DRGs have been utilized as a research target for chronic pain treatment [58], the association between SAHA and SCN9A and other downstream genes was examined in DRGs acquired from model mice. It was found that the protein level of SCN9A was down-regulated after SAHA, without remarkable changes in its mRNA level. Ubiquitination plays an essential part in the development of neuropathic pain [59]. Meantime, ubiquitin ligase NEDD4 regulates ubiquitination to impact the trafficking and degradation of proteins [60]. Furthermore, a prior study unveiled that the inhibition of NEDD4 up-regulated expression of SCN9A, thus contributing to an increase in the nociceptive neuronal hyperexcitability [61], which was in accordance with our observations that NEDD4 overexpression augmented the ubiquitination of SCN9A and then decreased SCN9A protein expression. These results implicated that SAHA might lighten pain hypersensitivity and anxiety/depression-like behaviors of SCI mice through regulation of NEDD4-mediated ubiquitination of SCN9A.

NEDD4-2 phosphorylation has been documented to participate in the development of chronic post-surgical pain [27]. Besides, it was revealed that histone acetylation regulates axon regeneration in SCI models and is closely related to neuropathic pain [62, 63]. Significantly, HDAC5 down-regulates NEDD4 expression by increasing the H3 acetylation during neuroblastoma cell differentiation [24]. It was discovered via our experiments that HDAC1 or HDAC5 knockdown promoted the enrichment of H3K27Ac in NEDD4 and that the knockdown of HDAC5 enhanced NEDD4 levels, which was similar to the effect of SAHA treatment. Furthermore, our rescue experiment results uncovered that NEDD4 silencing abrogated the improving impact of SAHA on pain hypersensitivity and anxiety/depression-like behaviors of SCI mice. Similarly, Hu et al. concluded in their research that the blockage of NEDD4 leads to depression-like behaviors in model rats [64].

To sum up, it was elucidated by our experimental data that SAHA ameliorated pain sensitization in central neuropathic pain after SCI through the HDAC5-NEDD4-SCN9A axis. These findings might offer credible data for the promotion of novel research directions on the treatment of central neuropathic pain. Additionally, our discovery that ITCH expression was up-regulated, together with NEDD4, after SAHA treatment, indicated the potential involvement of other ubiquitination-modifying proteins in the effects of SAHA on pain hypersensitivity and anxiety/depression-like behaviors of SCI mice. The related research should be further propelled.

Supplementary Information The online version contains supplementary material available at https://doi.org/10.1007/s11064-023-03913-z.

Acknowledgements Thanks to all the contributors.

Authors' contribution CW and RC conceived the ideas; designed the experiments. RC and XTZ performed the experiments. XTZ and XBZ analyzed the data. All authors provided critical materials. XTZ and XBZ wrote the manuscript. CW supervised the study. All the authors have read and approved the final version for publication.

Funding None.

Availability of data and materials The datasets used or analyzed during the current study are available from the corresponding author on reasonable request.

Declarations

Conflict of interest The authors report no relationships that could be construed as a conflict of interest.

References

1. Alizadeh A, Dyck SM, Karimi-Abdolrezaee S (2019) Traumatic spinal cord injury: an overview of pathophysiology, models and acute injury mechanisms. Front Neurol 10:282
2. Bradbury EJ, Burnside ER (2019) Moving beyond the glial scar for spinal cord repair. Nat Commun 10(1):3879
3. Qian J, Zhu W, Lu M et al (2017) D-beta-hydroxybutyrate promotes functional recovery and relieves pain hypersensitivity in mice with spinal cord injury. Br J Pharmacol 174(13):1961–1971
4. Viswanath O, Urits I, Burns J et al (2020) Central neuropathic mechanisms in pain signaling pathways: current evidence and recommendations. Adv Ther 37(5):1946–1959
5. Liu ZY, Song ZW, Guo SW et al (2019) CXCL12/CXCR4 signaling contributes to neuropathic pain via central sensitization mechanisms in a rat spinal nerve ligation model. CNS Neurosci Ther 25(9):922–936
6. Curatolo M, Muller M, Ashraf A et al (2015) Pain hypersensitivity and spinal nociceptive hypersensitivity in chronic pain: prevalence and associated factors. Pain 156(11):2373–2382
7. Liu S, Huang Q, He S et al (2019) Dermorphin [D-Arg2, Lys4] (1–4) amide inhibits below-level heat hypersensitivity in mice after contusive thoracic spinal cord injury. Pain 160(12):2710–2723
8. Mata-Bermudez A, Rios C, Burelo M et al (2021) Amantadine prevented hypersensitivity and decreased oxidative stress by NMDA receptor antagonism after spinal cord injury in rats. Eur J Pain 25(8):1839–1851
9. Niehaus JK, Taylor-Blake B, Loo L et al (2021) Spinal macrophages resolve nociceptive hypersensitivity after peripheral injury. Neuron 109(8):1274–1282
10. Wang P, Zhang Y, Xia Y et al (2021) MicroRNA-139-5p promotes functional recovery and reduces pain hypersensitivity in mice with spinal cord injury by targeting mammalian sterile 20-like kinase 1. Neurochem Res 46(2):349–357
11. Kumar V, Thakur JK, Prasad M (2021) Histone acetylation dynamics regulating plant development and stress responses. Cell Mol Life Sci 78(10):4467–4486
12. Sun C, An Q, Li R et al (2021) Calcitonin gene-related peptide induces the histone H3 lysine 9 acetylation in astrocytes associated with neuroinflammation in rats with neuropathic pain. CNS Neurosci Ther 27(11):1409–1424
13. Bondarev AD, Attwood MM, Jonsson J et al (2021) Recent developments of HDAC inhibitors: emerging indications and novel molecules. Br J Clin Pharmacol 87(12):4577–4597
14. Yang J, Gong C, Ke Q et al (2021) Insights into the function and clinical application of HDAC5 in cancer management. front Oncol 11:661620
15. Gu P, Pan Z, Wang XM et al (2018) Histone deacetylase 5 (HDAC5) regulates neuropathic pain through SRY-related HMG-box 10 (SOX10)-dependent mechanism in mice. Pain 159(3):526–539
16. Ho TCS, Chan AHY, Ganesan A (2020) Thirty years of HDAC inhibitors: 2020 insight and hindsight. J Med Chem 63(21):12460–12484
17. Chen C, Liu A, Lu Q et al (2022) HDAC6 inhibitor ACY-1215 improves neuropathic pain and its comorbidities in rats of peripheral nerve injury by regulating neuroinflammation. Chem Biol Interact 353:109803
18. Moertl S, Payer S, Kell R et al (2019) Comparison of radiosensitization by HDAC inhibitors CUDC-101 and SAHA in pancreatic cancer cells. Int J Mol Sci 20:13
19. Takada N, Nakamura Y, Ikeda K et al (2021) Treatment with histone deacetylase inhibitor attenuates peripheral inflammation-induced cognitive dysfunction and microglial activation: the effect of SAHA as a peripheral HDAC inhibitor. Neurochem Res 46(9):2285–2296
20. Borgonetti V, Galeotti N (2021) Combined inhibition of histone deacetylases and BET family proteins as epigenetic therapy for nerve injury-induced neuropathic pain. Pharmacol Res 165:105431
21. Cheng J, Deng Y, Zhou J (2021) Role of the Ubiquitin System in Chronic Pain. Front Mol Neurosci 14:674914
22. Gu H, Jan Fada B (2020) Specificity in Ubiquitination Triggered by Virus Infection. Int J Mol Sci 21(11):2
23. Rape M (2018) Ubiquitylation at the crossroads of development and disease. Nat Rev Mol Cell Biol 19(1):59–70
24. Sun Y, Liu PY, Scarlett CJ et al (2014) Histone deacetylase 5 blocks neuroblastoma cell differentiation by interacting with N-Myc. Oncogene 33(23):2987–2994
25. Yang Y, Luo M, Zhang K et al (2020) Nedd4 ubiquitylates VDAC2/3 to suppress erastin-induced ferroptosis in melanoma. Nat Commun 11(1):433
26. Laedermann CJ, Cachemaille M, Kirschmann G et al (2013) Dysregulation of voltage-gated sodium channels by ubiquitin ligase NEDD4-2 in neuropathic pain. J Clin Invest 123(7):3002–3013
27. Liu BW, Zhang J, Hong YS et al (2021) NGF-induced Nav1.7 upregulation contributes to chronic post-surgical pain by activating SGK1-dependent Nedd4–2 phosphorylation. Mol Neurobiol 58(3):964–982
28. Cai S, Moutal A, Yu J et al (2021) Selective targeting of NaV1.7 via inhibition of the CRMP2-Ubc9 interaction reduces pain in rodents. Sci Transl Med 13(619):1314
29. Chew LA, Bellampalli SS, Dustrude ET et al (2019) Mining the Nav1.7 interactome: opportunities for chronic pain therapeutics. Biochem Pharmacol 163:9–20
30. Niu HL, Liu YN, Xue DQ et al (2021) Inhibition of Nav1.7 channel by a novel blocker QLS-81 for alleviation of neuropathic pain. Acta Pharmacol Sin 42(8):1235–1247
31. McGrath JC, Lilley E (2015) Implementing guidelines on reporting research using animals (ARRIVE etc.): new requirements for publication in BJP. Br J Pharmacol 172(13):3189–3193
32. Charan J, Kantharia ND (2013) How to calculate sample size in animal studies? J Pharmacol Pharmacother 4(4):303–306
33. Krishna V, Andrews H, Jin X et al (2013) A contusion model of severe spinal cord injury in rats. J Vis Exp 78:2
34. Chaplan SR, Bach FW, Pogrel JW et al (1994) Quantitative assessment of tactile allodynia in the rat paw. J Neurosci Methods 53(1):55–63
35. Hargreaves K, Dubner R, Brown F et al (1988) A new and sensitive method for measuring thermal nociception in cutaneous hyperalgesia. Pain 32(1):77–88
36. Wen J, Xu Y, Yu Z et al (2022) The cAMP response element-binding protein/brain-derived neurotrophic factor pathway in anterior cingulate cortex regulates neuropathic pain and anxiodepression like behaviors in rats. Front Mol Neurosci 15:831151
37. Boinon L, Yu J, Madura CL et al (2022) Conditional knockout of CRMP2 in neurons, but not astrocytes, disrupts spinal nociceptive neurotransmission to control the initiation and maintenance of chronic neuropathic pain. Pain 163(2):e368–e381
38. Moreno AM, Aleman F, Catroli GF et al (2021) Long-lasting analgesia via targeted in situ repression of Na(V)1.7 in mice. Sci Transl Med 13:584
39. van Bemmelen MX, Rougier JS, Gavillet B et al (2004) Cardiac voltage-gated sodium channel Nav1.5 is regulated by Nedd4–2 mediated ubiquitination. Circ Res 95(3):284–291
40. Gwak YS, Hulsebosch CE (2011) GABA and central neuropathic pain following spinal cord injury. Neuropharmacology 60(5):799–808

41. Carlton SM, Du J, Tan HY et al (2009) Peripheral and central sensitization in remote spinal cord regions contribute to central neuropathic pain after spinal cord injury. Pain 147(1–3):265–276
42. Lin HC, Huang YH, Chao TH et al (2014) Gabapentin reverses central hypersensitivity and suppresses medial prefrontal cortical glucose metabolism in rats with neuropathic pain. Mol Pain 10:63
43. Smart KM, Blake C, Staines A et al (2012) Self-reported pain severity, quality of life, disability, anxiety and depression in patients classified with "nociceptive", "peripheral neuropathic" and "central sensitisation" pain. The discriminant validity of mechanisms-based classifications of low back (+/-leg) pain. Man Ther 17(2):119–125
44. Sato T, Verma S, Andrade CDC et al (2020) A FAK/HDAC5 signaling axis controls osteocyte mechanotransduction. Nat Commun 11(1):3282
45. He X, Zhang J, Guo Y et al (2022) Exosomal miR-9–5p derived from BMSCs alleviates apoptosis, inflammation and endoplasmic reticulum stress in spinal cord injury by regulating the HDAC5/FGF2 axis. Mol Immunol 145:97–108
46. Gu P, Fan T, Wong SSC et al (2021) Central endothelin-1 confers analgesia by triggering spinal neuronal histone deacetylase 5 (HDAC5) nuclear exclusion in peripheral neuropathic pain in mice. J Pain 22(4):454–471
47. Higuchi F, Uchida S, Yamagata H et al (2016) Hippocampal microRNA-124 enhances chronic stress resilience in mice. J Neurosci 36(27):7253–7267
48. Fujimoto T, Inoue-Mochita M, Iraha S et al (2021) Suberoylanilide hydroxamic acid (SAHA) inhibits transforming growth factor-beta 2-induced increases in aqueous humor outflow resistance. J Biol Chem 297(3):101070
49. Feng XL, Deng HB, Wang ZG et al (2019) Suberoylanilide hydroxamic acid triggers autophagy by influencing the mTOR pathway in the spinal dorsal horn in a rat neuropathic pain model. Neurochem Res 44(2):450–464
50. He XT, Hu XF, Zhu C et al (2020) Suppression of histone deacetylases by SAHA relieves bone cancer pain in rats via inhibiting activation of glial cells in spinal dorsal horn and dorsal root ganglia. J Neuroinflam 17(1):125
51. Meylan EM, Halfon O, Magistretti PJ et al (2016) The HDAC inhibitor SAHA improves depressive-like behavior of CRTC1-deficient mice: possible relevance for treatment-resistant depression. Neuropharmacology 107:111–121
52. Whittle N, Singewald N (2014) HDAC inhibitors as cognitive enhancers in fear, anxiety and trauma therapy: where do we stand? Biochem Soc Trans 42(2):569–581
53. Snyder LM, Ross SE, Belfer I (2014) An SCN9A variant, known to cause pain, is now found to cause itch. Pain 155(9):1677–1678
54. Grubinska B, Chen L, Alsaloum M et al (2019) Rat Na(V)1.7 loss-of-function genetic model: deficient nociceptive and neuropathic pain behavior with retained olfactory function and intra-epidermal nerve fibers. Mol Pain 15:174
55. Francois-Moutal L, Dustrude ET, Wang Y et al (2018) Inhibition of the Ubc9 E2 SUMO-conjugating enzyme-CRMP2 interaction decreases NaV1.7 currents and reverses experimental neuropathic pain. Pain 159(10):2115–2127
56. Bankar G, Goodchild SJ, Howard S et al (2018) Selective Na(V)1.7 antagonists with long residence time show improved efficacy against inflammatory and neuropathic pain. Cell Rep 24(12):3133–3145
57. Li Y, North RY, Rhines LD et al (2018) DRG voltage-gated sodium channel 1.7 is upregulated in paclitaxel-induced neuropathy in rats and in humans with neuropathic pain. J Neurosci 38(5):1124–1136
58. Berta T, Qadri Y, Tan PH et al (2017) Targeting dorsal root ganglia and primary sensory neurons for the treatment of chronic pain. Expert Opin Ther Targets 21(7):695–703
59. Sun L, Tong CK, Morgenstern TJ et al (2022) Targeted ubiquitination of sensory neuron calcium channels reduces the development of neuropathic pain. Proc Natl Acad Sci U S A 119(20):e2118129119
60. Donovan P, Poronnik P (2013) Nedd4 and Nedd4-2: ubiquitin ligases at work in the neuron. Int J Biochem Cell Biol 45(3):706–710
61. Laedermann CJ, Abriel H, Decosterd I (2015) Post-translational modifications of voltage-gated sodium channels in chronic pain syndromes. Front Pharmacol 6:263
62. Hutson TH, Kathe C, Palmisano I et al (2019) Cbp-dependent histone acetylation mediates axon regeneration induced by environmental enrichment in rodent spinal cord injury models. Sci Transl Med 11:487
63. Wang X, Shen X, Xu Y et al (2018) The etiological changes of acetylation in peripheral nerve injury-induced neuropathic hypersensitivity. Mol Pain 14:1744
64. Hu Y, Hong XY, Yang XF et al (2019) Inflammation-dependent ISG15 upregulation mediates MIA-induced dendrite damages and depression by disrupting NEDD4/Rap2A signaling. Biochim Biophys Acta Mol Basis Dis 6:1477–1489